Supplementary Information

Substituent directed selectivity in anion recognition by a new class of simple osmium-pyrazole derived receptor

Ankita Das, Prasenjit Mondal, Moumita Dasgupta, Nand Kishore* and Goutam Kumar Lahiri*

Department of Chemistry, Indian Institute of Technology Bombay, Powai, Mumbai-400076, India. E-mail: lahiri@chem.iitb.ac.in

Table S1 Experimental and DFT calculated selected bond angles (^{o}) for [**1**]ClO_4

Bond angles (^{o})	[**1**]ClO_4	
	X-ray	DFT
N1-Os1-N3	86.9(3)	87.14
N1-Os1-N4	90.5(3)	90.90
N1-Os1-N5	174.2(3)	172.96
N1-Os1-N6	95.9(3)	95.94
N3-Os1-N4	78.7(3)	77.99
N3-Os1-N5	98.2(3)	98.97
N3-Os1-N6	176.0(3)	176.37
N4-Os1-N5	93.2(3)	93.76
N4-Os1-N6	98.4(3)	100.00
N5-Os1-N6	79.2(3)	78.07
N1-Os1-Cl1	90.0(2)	87.92
N3-Os1-Cl1	95.7(2)	95.47
N4-Os1-Cl1	174.4(2)	173.41
N5-Os1-Cl1	86.7(2)	88.02
N6-Os1-Cl1	87.1(2)	86.55
N2-H2-Cl1	123.8	134.22
N2-H2-O1	136.5	-

Table S2 Experimental and DFT calculated selected bond angles (^{o}) for [**2**]ClO_4

Bond angles (^{o})	[**2**]ClO_4	
	X-ray	DFT
N1-Os1-N3	83.1(2)	86.52
N1-Os1-N4	93.5(2)	94.75
N1-Os1-N5	177.3(3)	172.51
N1-Os1-N6	99.0(2)	96.05
N3-Os1-N4	78.0(2)	77.88
N3-Os1-N5	99.6(2)	99.52
N3-Os1-N6	177.7(2)	176.99
N4-Os1-N5	86.5(2)	90.85
N4-Os1-N6	101.0(3)	100.31
N5-Os1-N6	78.3(2)	78.03
N1-Os1-Cl1	87.66(17)	87.91
N3-Os1-Cl1	96.00(17)	95.16
N4-Os1-Cl1	173.70(19)	172.36
N5-Os1-Cl1	92.59(18)	87.15
N6-Os1-Cl1	84.92(18)	86.49
N2-H2-Cl1	114.9	136.27
N2-H2-O1	155.9	-

Table S3 DFT calculated selected MO compositions for $\mathbf{1}^n$ and $\mathbf{2}^n$

Complex	MO	Fragments	% Contribution
$\mathbf{1}^{3+}$ (S = 1)	β -LUMO	Os/bpy/Cl	67/14/12
$\mathbf{1}^{2+}$ (S = 1/2)	β -HOMO	Os/bpy/HL_1	63/15/11
	β -LUMO	Os/bpy/Cl	71/17/09
$\mathbf{1}^{+}$ (S = 0)	HOMO	Os/Cl/bpy	64/17/16
	LUMO	bpy	89
1 (S = 1/2)	SOMO	bpy	91
$\mathbf{2}^{3+}$ (S = 1)	β -LUMO	Os/HL_2	59/24
$\mathbf{2}^{2+}$ (S = 1/2)	β -HOMO	Os/HL_2	50/38
	β -LUMO	Os/bpy	70/19
$\mathbf{2}^{+}$ (S = 0)	HOMO	Os/bpy/Cl	69/15/11
	LUMO	bpy	88
2 (S = 1/2)	SOMO	bpy	91

Table S4 Composition and energies of selected molecular orbitals of **1**$^{+}$ (*S*=0)

MO	Energy(eV)	Composition			
		Os	HL_1	bpy	Cl
HOMO–5	–9.696	0.06	0.04	0.37	0.53
HOMO–4	–9.654	0.10	0.03	0.32	0.56
HOMO–3	–9.483	0.03	0.02	0.65	0.30
HOMO–2	–7.919	0.66	0.10	0.20	0.03
HOMO–1	–7.749	0.61	0.02	0.20	0.16
HOMO	–7.547	0.64	0.02	0.16	0.17
LUMO	–4.818	0.09	0.01	0.89	0.01
LUMO+1	–4.660	0.10	0.01	0.88	0.01
LUMO+2	–4.032	0.03	0.01	0.96	0.00
LUMO+3	–3.766	0.05	0.00	0.94	0.00
LUMO+4	–3.742	0.04	0.01	0.95	0.00
LUMO+5	–3.591	0.06	0.02	0.92	0.00

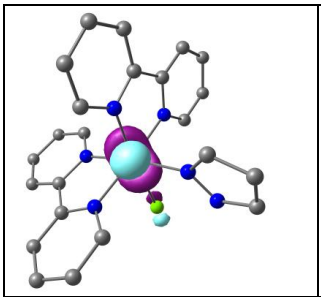	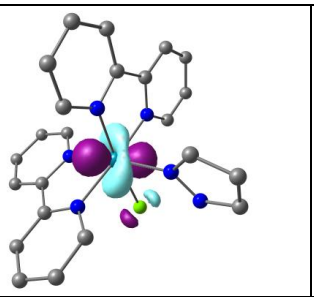	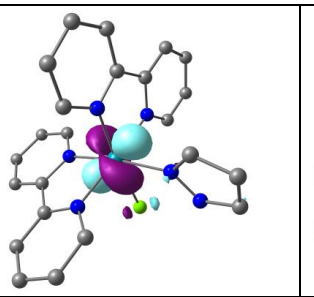	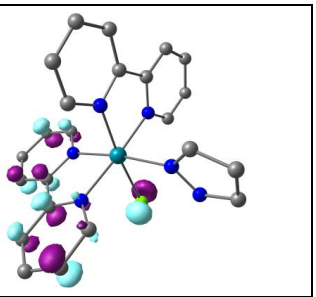
HOMO	HOMO–1	HOMO–2	HOMO–3
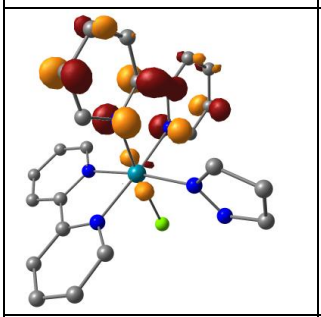	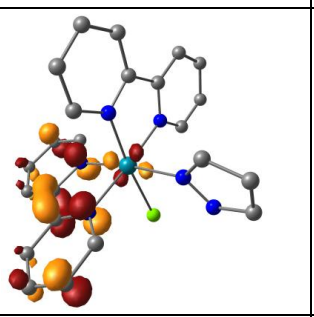	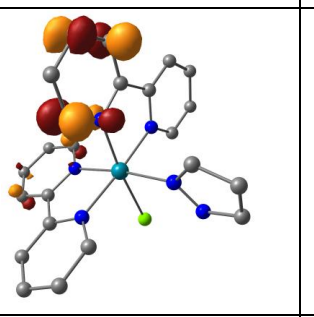	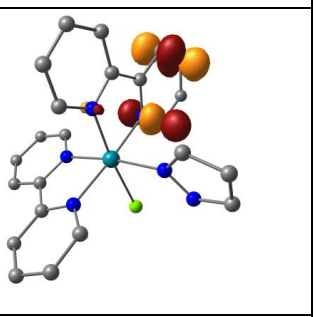
LUMO	LUMO+1	LUMO+2	LUMO+3

Table S5 Composition and energies of selected molecular orbitals of $\mathbf{1}^{2+}$ (S=1/2)

MO	Energy(eV)	Composition			
		Os	HL_1	bpy	Cl
		α-spin			
HOMO–5	–13.136	0.15	0.66	0.15	0.03
HOMO–4	–13.023	0.03	0.12	0.84	0.02
HOMO–3	–12.846	0.03	0.03	0.87	0.07
HOMO–2	–12.621	0.42	0.11	0.20	0.27
HOMO–1	–12.279	0.56	0.09	0.16	0.19
SOMO	–12.193	0.59	0.15	0.15	0.11
LUMO	–8.327	0.06	0.01	0.92	0.00
LUMO+1	–8.108	0.06	0.00	0.92	0.01
LUMO+2	–7.375	0.02	0.01	0.97	0.00
LUMO+3	–7.056	0.03	0.00	0.97	0.00
LUMO+4	–6.985	0.04	0.00	0.96	0.00
LUMO+5	–6.944	0.02	0.01	0.97	0.00
		β-spin			
HOMO–5	–13.422	0.08	0.06	0.20	0.66
HOMO–4	–13.034	0.04	0.53	0.38	0.05
HOMO–3	–13.005	0.03	0.28	0.65	0.04
HOMO–2	–12.825	0.00	0.01	0.97	0.02
HOMO–1	–12.020	0.61	0.08	0.16	0.15
HOMO	–11.938	0.63	0.11	0.15	0.11
LUMO	–9.860	0.71	0.03	0.17	0.09
LUMO+1	–8.280	0.08	0.01	0.91	0.01
LUMO+2	–8.081	0.07	0.00	0.91	0.01
LUMO+3	–7.339	0.03	0.01	0.96	0.00
LUMO+4	–7.014	0.03	0.01	0.96	0.00
LUMO+5	–6.970	0.04	0.00	0.96	0.00

α-spin			
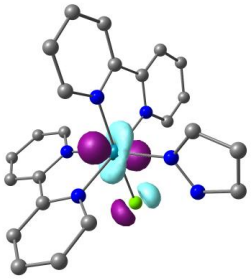	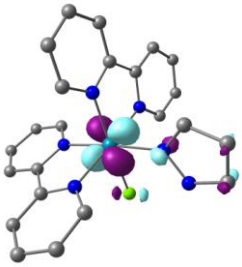	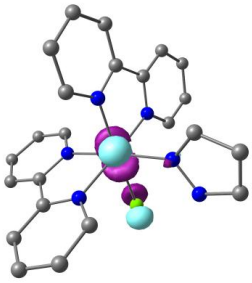	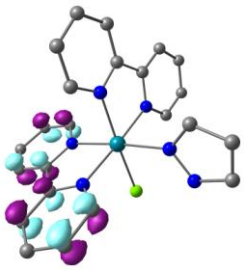
SOMO	HOMO–1	HOMO–2	HOMO–3
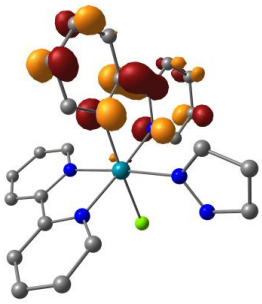	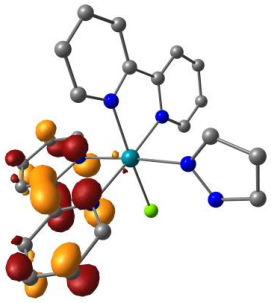	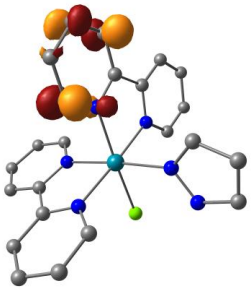	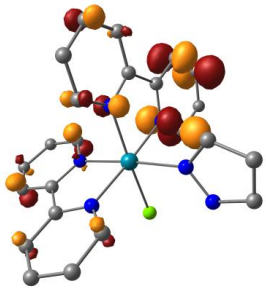
LUMO	LUMO+1	LUMO+2	LUMO+3
β-spin			
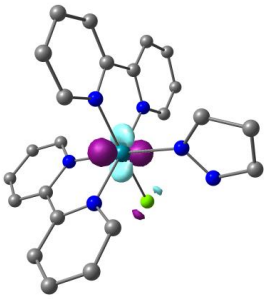	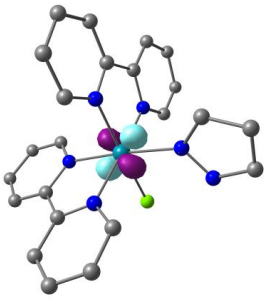	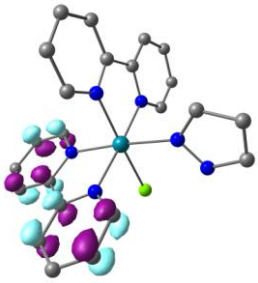	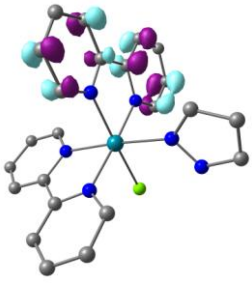
HOMO	HOMO–1	HOMO–2	HOMO–3
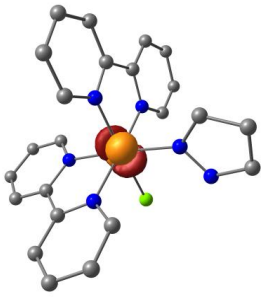	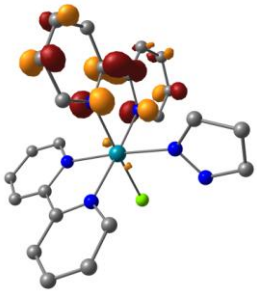	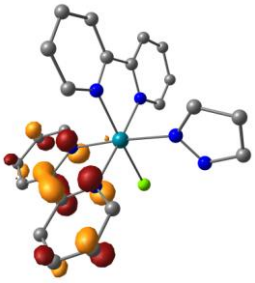	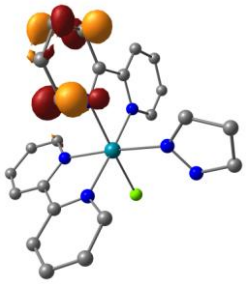
LUMO	LUMO+1	LUMO+2	LUMO+3

Table S6 Composition and energies of selected molecular orbitals of $\mathbf{1}^{3+}$ (S=1)

MO	Energy(eV)	Composition			
		Os	HL_1	bpy	Cl
		α-spin			
HOMO–5	–17.015	0.39	0.02	0.27	0.32
HOMO–4	–16.858	0.23	0.63	0.11	0.04
HOMO–3	–16.676	0.46	0.06	0.25	0.22
HOMO–2	–16.343	0.20	0.72	0.06	0.02
SOMO 2	–16.129	0.01	0.01	0.97	0.01
SOMO 1	–16.050	0.01	0.00	0.99	0.00
LUMO	–11.537	0.05	0.01	0.94	0.00
LUMO+1	–11.448	0.04	0.00	0.94	0.01
LUMO+2	–10.910	0.46	0.03	0.32	0.19
LUMO+3	–10.479	0.03	0.02	0.95	0.00
LUMO+4	–10.402	0.34	0.10	0.56	0.00
LUMO+5	–10.249	0.06	0.02	0.92	0.00
		β-spin			
HOMO–5	–17.225	0.02	0.01	0.55	0.42
HOMO–4	–17.091	0.05	0.63	0.31	0.01
HOMO–3	–16.576	0.24	0.61	0.14	0.01
HOMO–2	–16.143	0.04	0.01	0.94	0.01
HOMO–1	–16.051	0.09	0.05	0.83	0.03
HOMO	–16.007	0.37	0.26	0.26	0.12
LUMO	–14.358	0.67	0.07	0.14	0.12
LUMO+1	–14.101	0.68	0.06	0.13	0.13
LUMO+2	–11.487	0.06	0.01	0.93	0.00
LUMO+3	–11.347	0.32	0.00	0.92	0.01
LUMO+4	–10.470	0.28	0.01	0.55	0.12
LUMO+5	–10.431	0.05	0.03	0.58	0.11

α-spin			
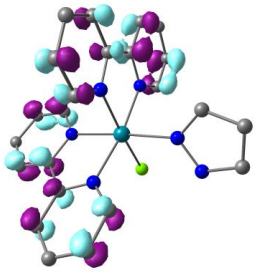	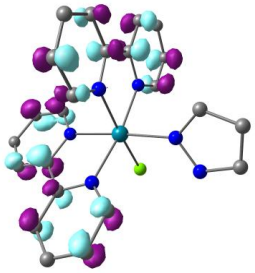	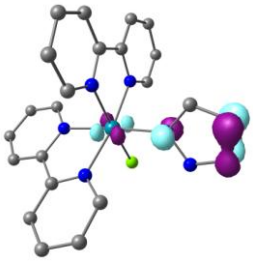	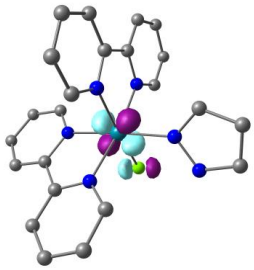
SOMO 1	SOMO 2	HOMO–2	HOMO–3
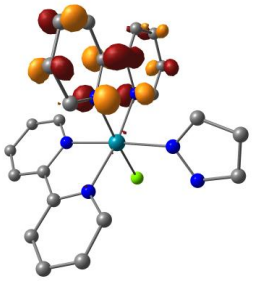	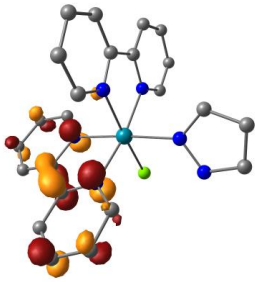	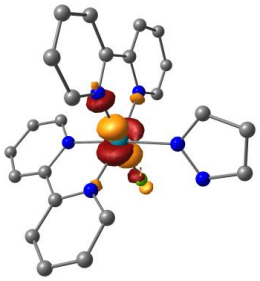	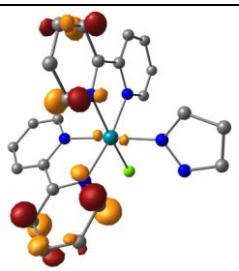
LUMO	LUMO+1	LUMO+2	LUMO+3
β-spin			
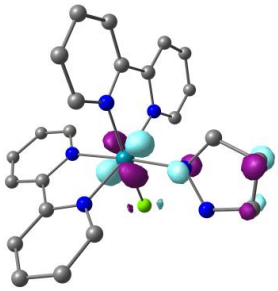	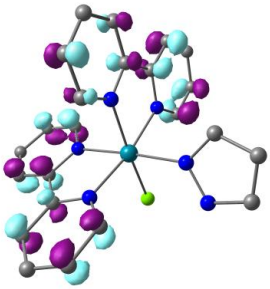	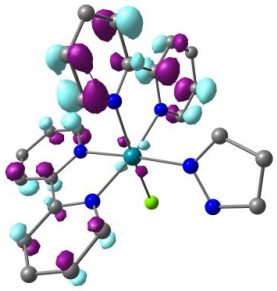	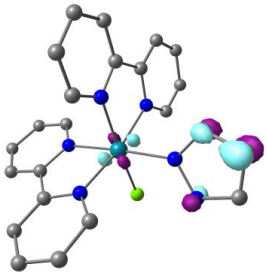
HOMO	HOMO–1	HOMO–2	HOMO–3
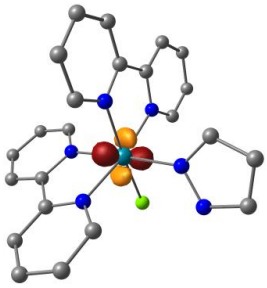	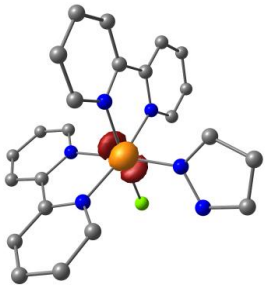	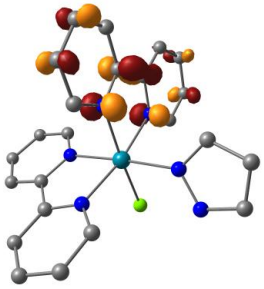	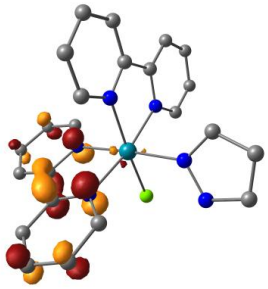
LUMO	LUMO+1	LUMO+2	LUMO+3

Table S7 Composition and energies of selected molecular orbitals of **1** (*S*=1/2)

MO	Energy(eV)	Composition			
		Os	HL_1	bpy	Cl
		α-spin			
HOMO–5	–6.418	0.00	0.01	0.91	0.08
HOMO–4	–6.291	0.00	0.00	0.99	0.00
HOMO–3	–4.606	0.69	0.08	0.21	0.02
HOMO–2	–4.485	0.67	0.01	0.21	0.11
HOMO–1	–4.262	0.72	0.03	0.16	0.09
SOMO 1	–2.342	0.08	0.01	0.91	0.01
LUMO	–1.625	0.13	0.01	0.85	0.01
LUMO+1	–0.669	0.04	0.01	0.94	0.00
LUMO+2	–0.526	0.03	0.01	0.96	0.00
LUMO+3	–0.346	0.04	0.02	0.95	0.00
LUMO+4	–0.293	0.09	0.01	0.90	0.00
LUMO+5	0.155	0.06	0.89	0.04	0.00
		β-spin			
HOMO–5	–6.632	0.06	0.02	0.16	0.75
HOMO–4	–6.293	0.00	0.00	0.93	0.06
HOMO–3	–6.079	0.01	0.00	0.98	0.00
HOMO–2	–4.577	0.69	0.05	0.20	0.07
HOMO–1	–4.393	0.70	0.05	0.19	0.05
HOMO	–4.237	0.72	0.02	0.16	0.10
LUMO	–1.314	0.09	0.00	0.90	0.01
LUMO+1	–1.072	0.09	0.02	0.89	0.00
LUMO+2	–0.618	0.05	0.01	0.93	0.01
LUMO+3	–0.440	0.03	0.01	0.96	0.00
LUMO+4	–0.256	0.06	0.02	0.92	0.00
LUMO+5	–0.158	0.05	0.01	0.94	0.00

α-spin			
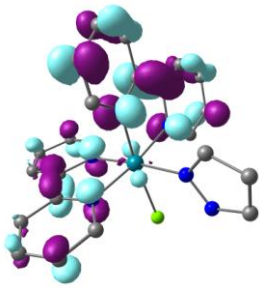	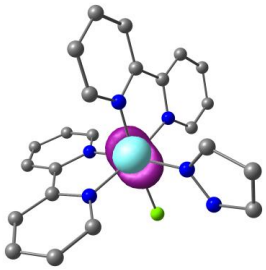	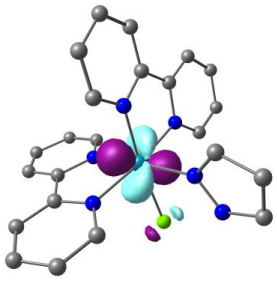	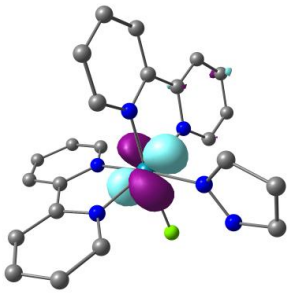
SOMO 1	HOMO–1	HOMO–2	HOMO–3
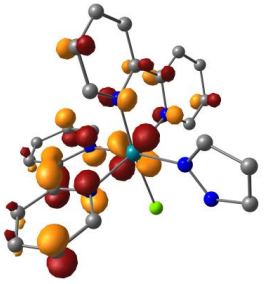	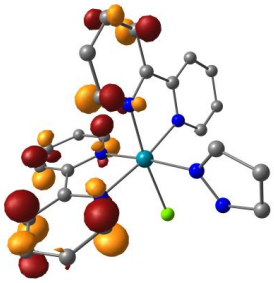	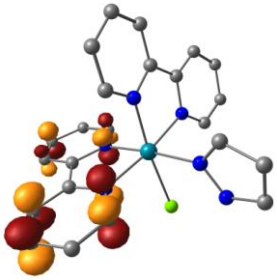	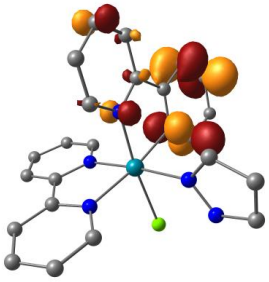
LUMO	LUMO+1	LUMO+2	LUMO+3
β-spin			
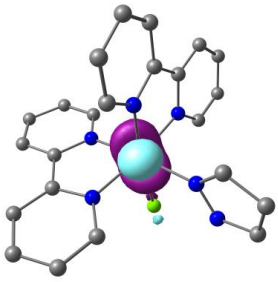	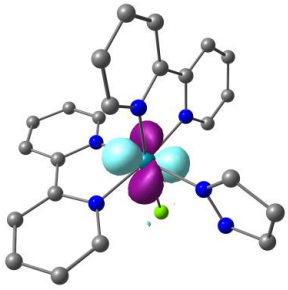	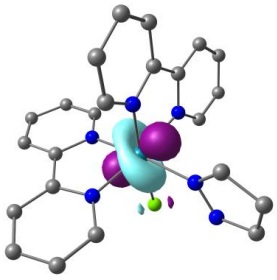	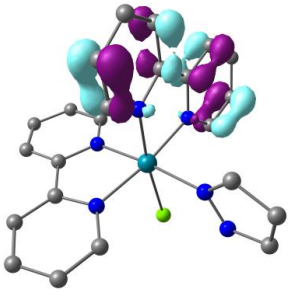
HOMO	HOMO–1	HOMO–2	HOMO–3
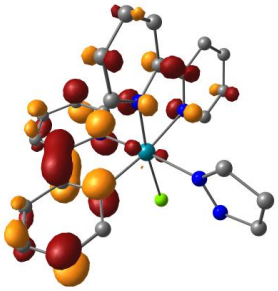	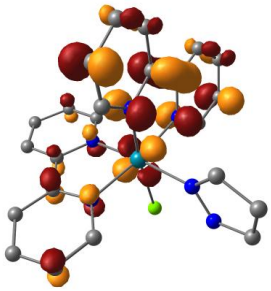	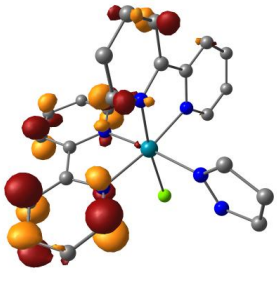	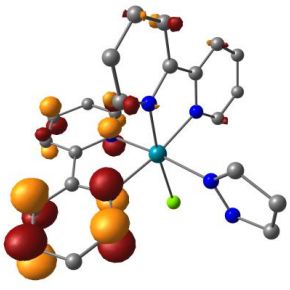
LUMO	LUMO+1	LUMO+2	LUMO+3

Table S8 Composition and energies of selected molecular orbitals of **2**$^{+}$ (*S*=0)

MO	Energy(eV)	Composition			
		Os	HL_2	bpy	Cl
HOMO–5	–9.607	0.06	0.39	0.46	0.09
HOMO–4	–9.547	0.01	0.06	0.75	0.18
HOMO–3	–9.357	0.01	0.69	0.23	0.07
HOMO–2	–7.870	0.62	0.07	0.21	0.10
HOMO–1	–7.737	0.66	0.07	0.18	0.08
HOMO	–7.593	0.69	0.04	0.15	0.11
LUMO	–4.885	0.10	0.02	0.88	0.01
LUMO+1	–4.673	0.09	0.00	0.89	0.01
LUMO+2	–4.035	0.03	0.02	0.94	0.00
LUMO+3	–3.714	0.04	0.02	0.94	0.00
LUMO+4	–3.686	0.05	0.00	0.94	0.00
LUMO+5	–3.593	0.05	0.01	0.94	0.00

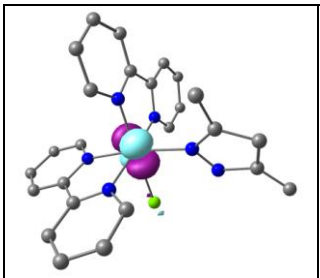	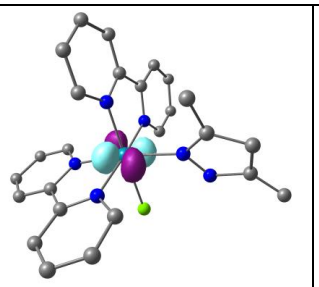	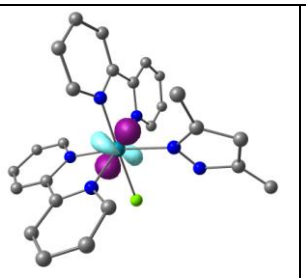	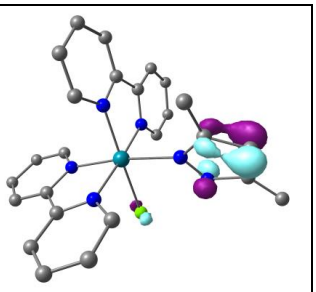
HOMO	HOMO–1	HOMO–2	HOMO–3
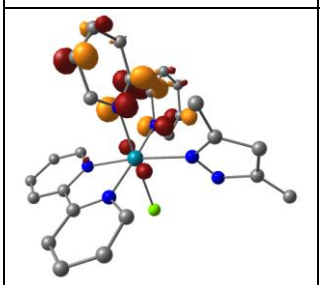	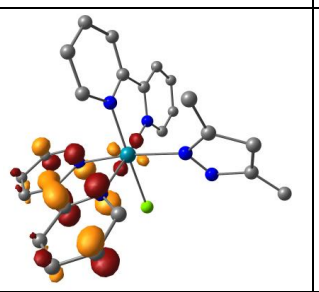	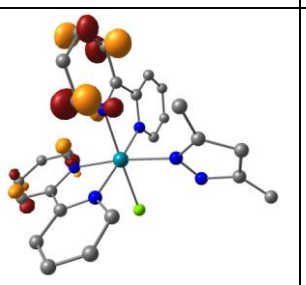	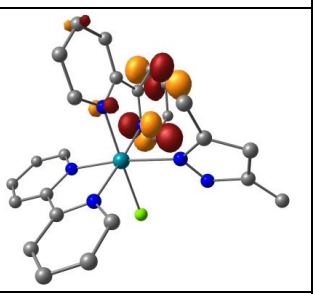
LUMO	LUMO+1	LUMO+2	LUMO+3

Table S9 Composition and energies of selected molecular orbitals of **2**$^{2+}$ (*S*=1/2)

MO	Energy(eV)	Composition			
		Os	HL_2	bpy	Cl
		α-spin			
HOMO−5	−12.939	0.12	0.12	0.73	0.03
HOMO−4	−12.799	0.06	0.02	0.84	0.08
HOMO−3	−12.595	0.38	0.23	0.22	0.17
HOMO−2	−12.400	0.20	0.55	0.08	0.17
HOMO−1	−12.193	0.57	0.05	0.15	0.23
SOMO	−11.843	0.41	0.49	0.10	0.01
LUMO	−8.264	0.07	0.01	0.92	0.00
LUMO+1	−8.047	0.06	0.00	0.93	0.01
LUMO+2	−7.323	0.02	0.02	0.96	0.00
LUMO+3	−6.996	0.03	0.01	0.96	0.00
LUMO+4	−6.933	0.03	0.01	0.95	0.00
LUMO+5	−6.880	0.02	0.01	0.97	0.00
		β-spin			
HOMO−5	−13.010	0.12	0.29	0.58	0.00
HOMO−4	−12.883	0.16	0.34	0.47	0.02
HOMO−3	−12.769	0.00	0.00	0.99	0.01
HOMO−2	−12.406	0.08	0.85	0.04	0.04
HOMO−1	−11.930	0.63	0.02	0.16	0.20
HOMO	−11.674	0.50	0.38	0.12	0.01
LUMO	−9.761	0.70	0.02	0.19	0.10
LUMO+1	−8.189	0.09	0.01	0.89	0.01
LUMO+2	−8.024	0.07	0.00	0.92	0.01
LUMO+3	−7.277	0.03	0.02	0.95	0.00
LUMO+4	−6.965	0.03	0.01	0.95	0.00
LUMO+5	−6.913	0.04	0.01	0.95	0.00

α-spin			
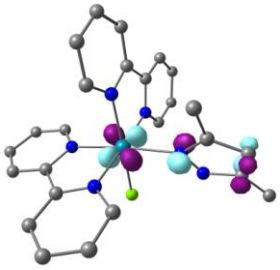	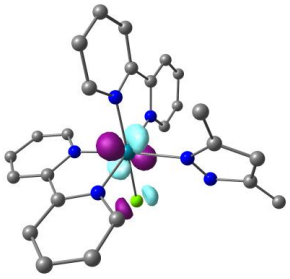	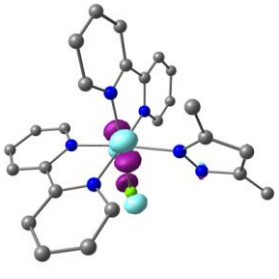	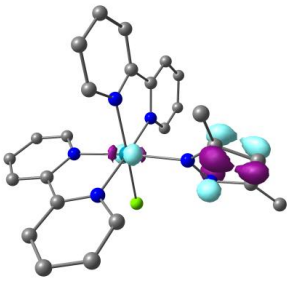
SOMO	HOMO–1	HOMO–2	HOMO–3
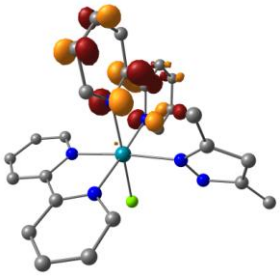	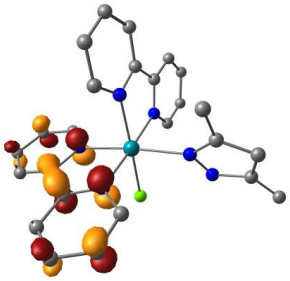	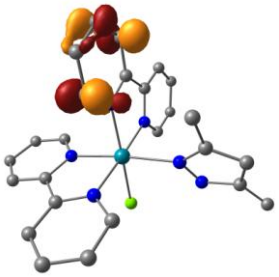	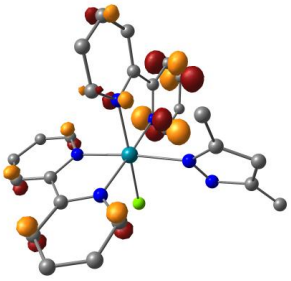
LUMO	LUMO+1	LUMO+2	LUMO+3
β-spin			
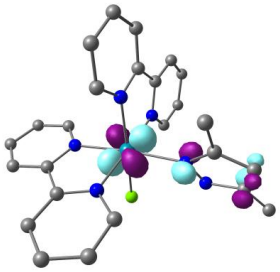	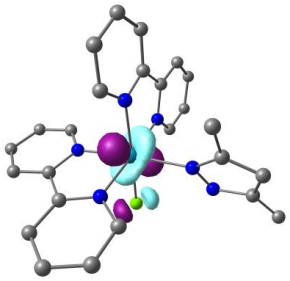	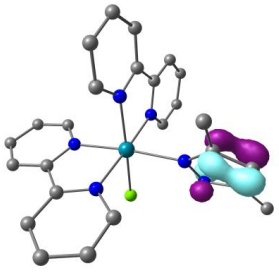	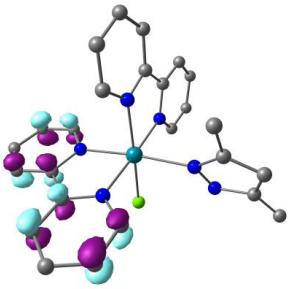
HOMO	HOMO–1	HOMO–2	HOMO–3
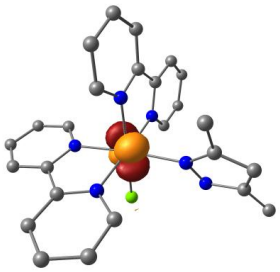	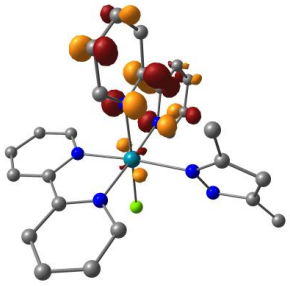	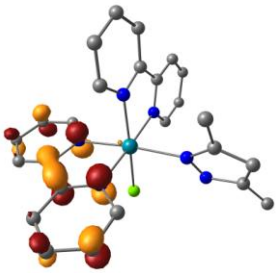	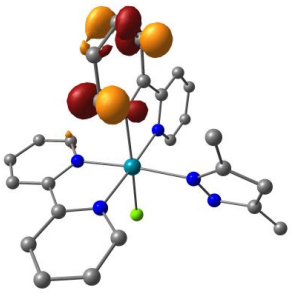
LUMO	LUMO+1	LUMO+2	LUMO+3

Table S10 Composition and energies of selected molecular orbitals of $\mathbf{2}^{3+}$ (S=1)

MO	Energy(eV)	Composition			
		Os	HL_2	bpy	Cl
		α-spin			
HOMO–5	–16.533	0.40	0.09	0.20	0.09
HOMO–4	–16.312	0.20	0.63	0.11	0.06
HOMO–3	–16.278	0.45	0.07	0.21	0.27
HOMO–2	–16.040	0.13	0.64	0.22	0.00
SOMO 2	–15.958	0.06	0.24	0.66	0.03
SOMO 1	–15.787	0.01	0.00	0.98	0.00
LUMO	–11.390	0.05	0.01	0.94	0.00
LUMO+1	–11.162	0.05	0.00	0.94	0.01
LUMO+2	–10.498	0.44	0.05	0.33	0.18
LUMO+3	–10.326	0.04	0.03	0.92	0.01
LUMO+4	–10.138	0.28	0.08	0.64	0.00
LUMO+5	–10.093	0.22	0.05	0.72	0.01
		β-spin			
HOMO–5	–16.910	0.03	0.02	0.48	0.47
HOMO–4	–16.496	0.18	0.64	0.18	0.00
HOMO–3	–16.093	0.27	0.54	0.13	0.06
HOMO–2	–16.001	0.03	0.06	0.90	0.01
HOMO–1	–15.791	0.00	0.00	0.99	0.00
HOMO	–15.657	0.42	0.28	0.13	0.16
LUMO	–14.085	0.59	0.24	0.13	0.05
LUMO+1	–13.682	0.68	0.01	0.14	0.17
LUMO+2	–11.275	0.07	0.01	0.91	0.00
LUMO+3	–11.108	0.06	0.00	0.93	0.01
LUMO+4	–10.283	0.03	0.02	0.95	0.00
LUMO+5	–10.120	0.24	0.04	0.62	0.10

α-spin			
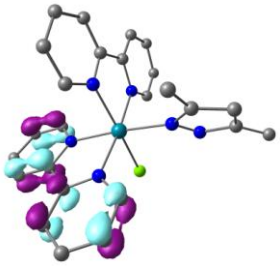	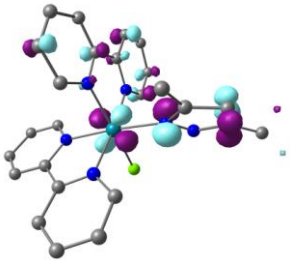	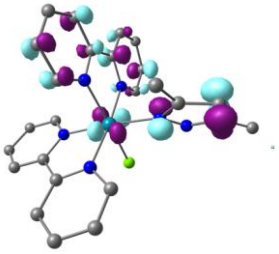	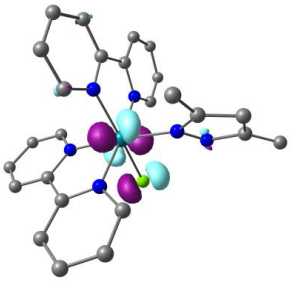
SOMO 1	SOMO 2	HOMO–2	HOMO–3
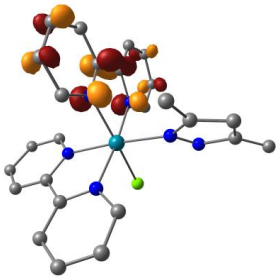	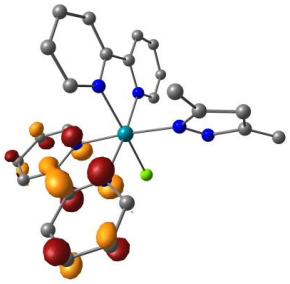	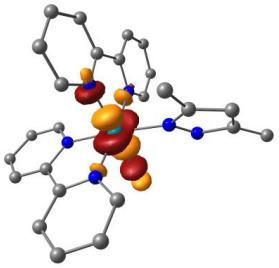	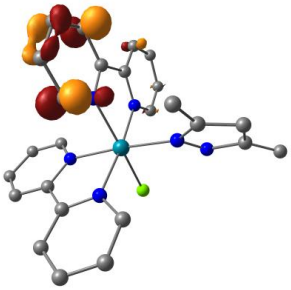
LUMO	LUMO+1	LUMO+2	LUMO+3
β-spin			
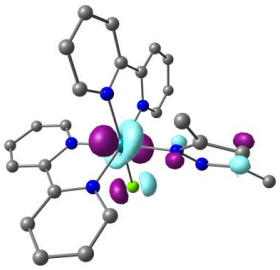	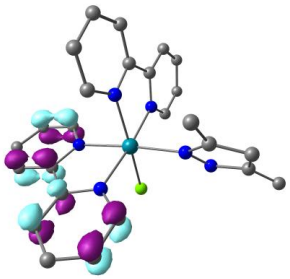	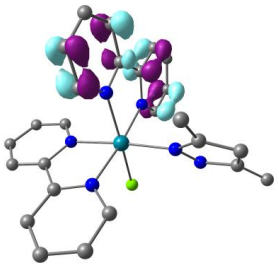	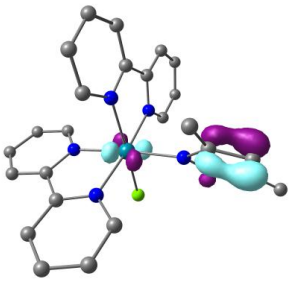
HOMO	HOMO–1	HOMO–2	HOMO–3
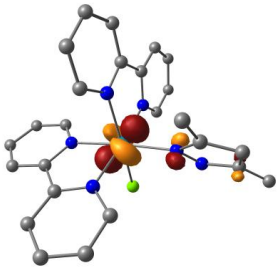	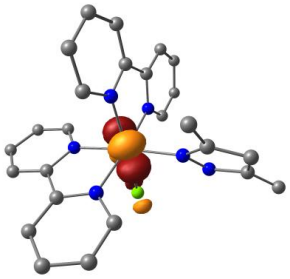	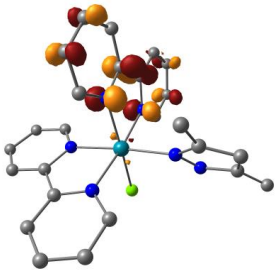	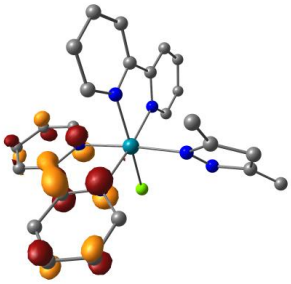
LUMO	LUMO+1	LUMO+2	LUMO+3

Table S11 Composition and energies of selected molecular orbitals of **2** (*S*=1/2)

MO	Energy(eV)	Composition			
		Os	HL_2	bpy	Cl
		α-spin			
HOMO–5	–6.376	0.00	0.01	0.87	0.03
HOMO–4	–6.270	0.00	0.03	0.97	0.08
HOMO–3	–4.518	0.71	0.10	0.18	0.17
HOMO–2	–4.481	0.65	0.02	0.23	0.17
HOMO–1	–4.212	0.72	0.02	0.16	0.23
SOMO	–2.308	0.08	0.01	0.91	0.01
LUMO	–1.606	0.13	0.01	0.85	0.01
LUMO+1	–0.635	0.04	0.03	0.92	0.00
LUMO+2	–0.491	0.03	0.01	0.96	0.00
LUMO+3	–0.333	0.04	0.01	0.95	0.00
LUMO+4	–0.273	0.09	0.03	0.88	0.00
LUMO+5	0.253	0.04	0.92	0.04	0.00
		β-spin			
HOMO–5	–6.525	0.04	0.18	0.15	0.63
HOMO–4	–6.242	0.00	0.01	0.92	0.07
HOMO–3	–6.067	0.01	0.02	0.97	0.00
HOMO–2	–4.509	0.67	0.05	0.20	0.09
HOMO–1	–4.391	0.73	0.07	0.18	0.03
HOMO	–4.169	0.71	0.01	0.17	0.10
LUMO	–1.262	0.08	0.00	0.90	0.01
LUMO+1	–1.069	0.09	0.03	0.88	0.00
LUMO+2	–0.581	0.05	0.03	0.92	0.01
LUMO+3	–0.409	0.04	0.01	0.95	0.00
LUMO+4	–0.229	0.05	0.01	0.94	0.00
LUMO+5	–0.160	0.06	0.03	0.91	0.00

α-spin			
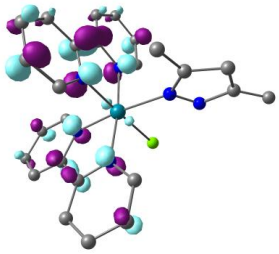	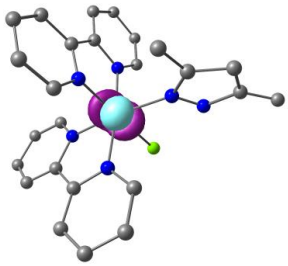	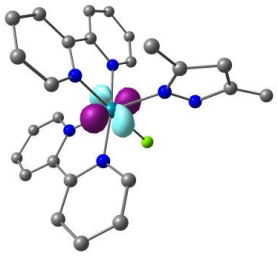	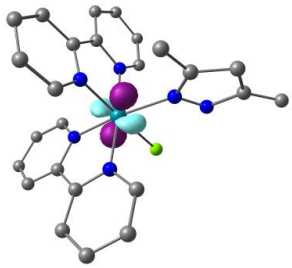
SOMO	HOMO–1	HOMO–2	HOMO–3
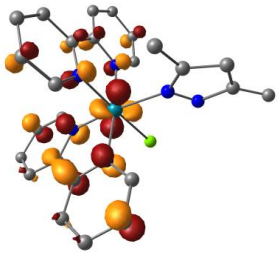	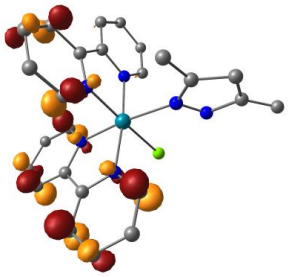	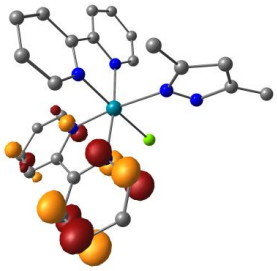	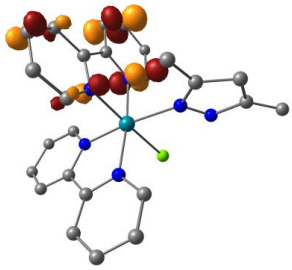
LUMO	LUMO+1	LUMO+2	LUMO+3
β-spin			
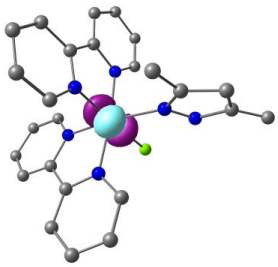	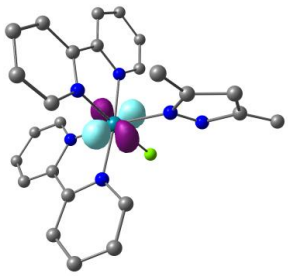	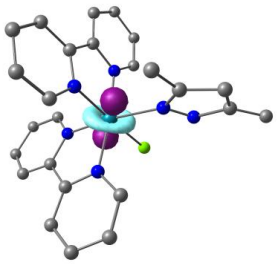	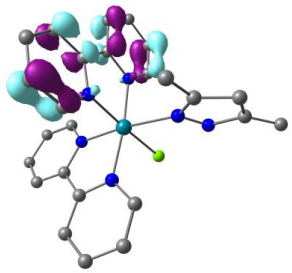
HOMO	HOMO–1	HOMO–2	HOMO–3
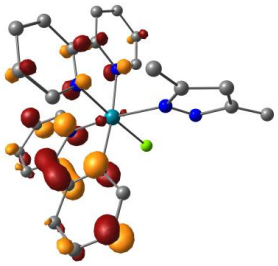	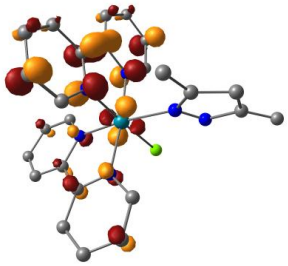	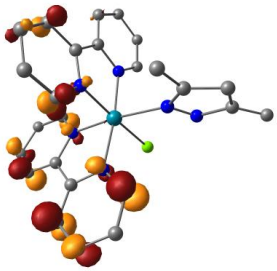	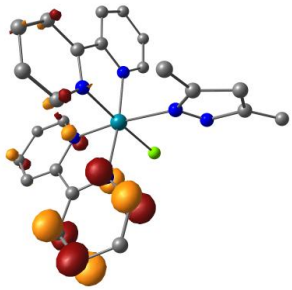
LUMO	LUMO+1	LUMO+2	LUMO+3

Table S12 DFT calculated Mulliken spin densities in the paramagnetic states of $\mathbf{1}^{n}$ and $\mathbf{2}^{n}$

Complex	Os1	HL	bpy	Cl
$\mathbf{1}^{3+}$ (S=1)	1.497	0.129	0.096	0.278
$\mathbf{1}^{2+}$ (S=1/2)	0.893	0.014	0.007	0.087
1 (S=1/2)	-0.058	0.002	1.055	0.001
$\mathbf{2}^{3+}$ (S=1)	1.427	0.291	0.076	0.204
$\mathbf{2}^{2+}$ (S=1/2)	0.888	-0.013	0.016	0.106
2 (S=1/2)	-0.056	0.001	1.062	0.002

Table S13 TD-DFT ((U)B3LYP/CPCM/CH_3CN) calculated electronic transitions for $\mathbf{1}^n$ and $\mathbf{2}^n$

λ /nm (expt.) (ε /dm^{3}mol^{-1} cm^{-1})	λ /nm (DFT) (f)	Transition	Character
		$\mathbf{1}^{2+}$ (S=1/2)	
518(3180)	517(0.003)	HOMO-2(β)→LUMO(β)(0.99)	bpy(π)→Os(dπ)
485(4760)	462(0.011)	HOMO-4(β)→LUMO(β)(0.97)	HL_1(π)/bpy(π)→Os(dπ)
383(20340)	365(0.032)	HOMO-1(α)→LUMO+1(α)(0.70)	Os(dπ)/Cl(π)→bpy(π*)
287(94310)	271(0.073)	HOMO-5(α)→LUMO(α)(0.35)	HL_1(π)/bpy(π)→bpy(π*)
		HOMO-8(β)→LUMO+1(β)(0.15)	Cl(π)/bpy(π)→bpy(π*)
	260(0.051)	HOMO-8(β)→LUMO+1(β)(0.31)	bpy(π)/Cl(π)→bpy(π*)
		HOMO-10(α)→LUMO(α)(0.21)	bpy(π)→bpy(π*)
		$\mathbf{1}^{+}$ (S=0)	
724(7970)	612(0.008)	HOMO→LUMO(0.68)	Os(dπ)/Cl(π)→bpy(π*)
	598(0.002)	HOMO→LUMO+1(0.68)	Os(dπ)/Cl(π)→bpy(π*)
520(29330)	491(0.193)	HOMO-2→LUMO(0.59)	Os(dπ)/bpy(π)→bpy(π*)
427(25760)	463(0.025)	HOMO-2→LUMO+1(0.58)	Os(dπ)/bpy(π)→bpy(π*)
	368(0.031)	HOMO-2→LUMO+2(0.55)	Os(dπ)/bpy(π)→bpy(π*)
355(29820)	322(0.097)	HOMO-2→LUMO+5(0.44)	Os(dπ)/bpy(π)→bpy(π*)
		HOMO-2→LUMO+3(0.26)	Os(dπ)/bpy(π)→bpy(π*)
	361(0.134)	HOMO-1→LUMO+3(0.46)	Os(dπ)/Cl(π)→bpy(π*)
		HOMO-2→LUMO+2(0.15)	Os(dπ)/bpy(π)→bpy(π*)
294(186320)	278(0.695)	HOMO-3→LUMO+1(0.51)	bpy(π)/Cl(π)→bpy(π*)
		$\mathbf{2}^{2+}$ (S=1/2)	
522(2060)	517(0.003)	HOMO-3(β)→LUMO(β)(0.99)	bpy(π)→Os(dπ)
490(3890)	491(0.011)	HOMO-5(β)→LUMO(β)(0.87)	bpy(π)/HL_2(π)→Os(dπ)
387(14760)	390(0.031)	SOMO(α)→LUMO(α)(0.59)	HL_2(π)/Os(dπ)→bpy(π*)
	426(0.013)	HOMO(β)→LUMO+2(β)(0.58)	Os(dπ)/HL_2(π)→bpy(π*)
286(71130)	276(0.122)	HOMO-8(α)→LUMO+1(α)(0.33)	bpy(π)→bpy(π*)
		HOMO-4(α)→LUMO+1(α)(0.20)	Cl(π)/bpy(π)→bpy(π*)
		$\mathbf{2}^{+}$ (S=0)	
734(7210)	610(0.007)	HOMO→LUMO(0.68)	Os(dπ)/bpy(π)→bpy(π*)
	604(0.003)	HOMO→LUMO+1(0.68)	Os(dπ)/bpy(π)→bpy(π*)
524(24550)	499(0.168)	HOMO-2→LUMO(0.51)	Os(dπ)/bpy(π)→bpy(π*)
	540(0.004)	HOMO-1→LUMO(0.47)	Os(dπ)/bpy(π)→bpy(π*)
		HOMO-2→LUMO+1(0.36)	Os(dπ)/bpy(π)→bpy(π*)
430(21690)	410(0.001)	HOMO-1→LUMO+2(0.67)	Os(dπ)/bpy(π)→bpy(π*)
355(23760)	360(0.008)	HOMO-1→LUMO+5(0.62)	Os(dπ)/bpy(π)→bpy(π*)
296(147200)	279(0.309)	HOMO-5→LUMO+1(0.52)	bpy(π)/HL_2(π)→bpy(π*)
	287(0.053)	HOMO-4→LUMO(0.42)	bpy(π)/Cl(π)→bpy(π*)
		HOMO-4→LUMO+1(0.22)	bpy(π)/Cl(π)→bpy(π*)

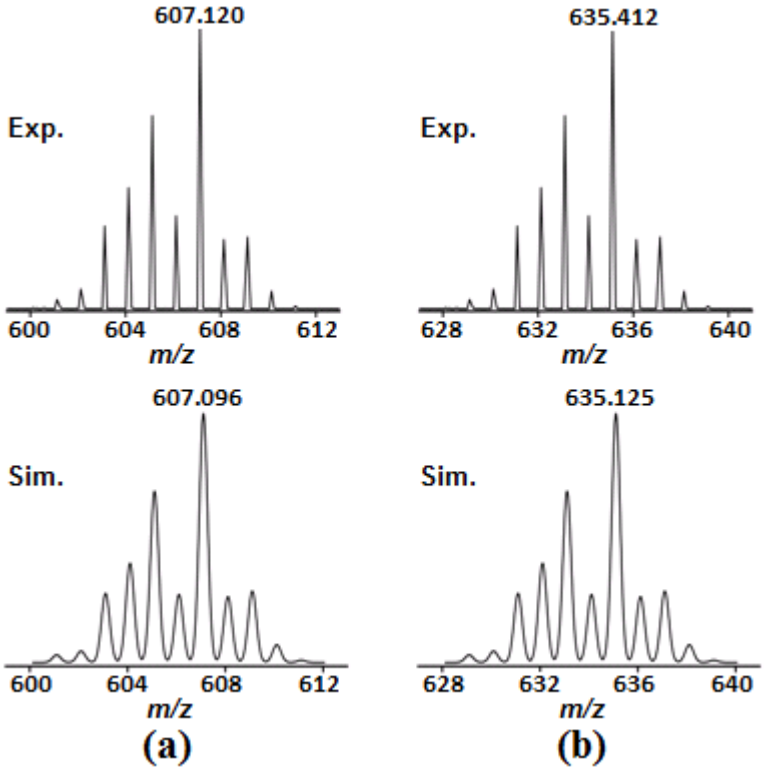

Fig. S1 ESI-MS of (a) [**1**]ClO_4 and (b) [**2**]ClO_4 in CH_3CN.

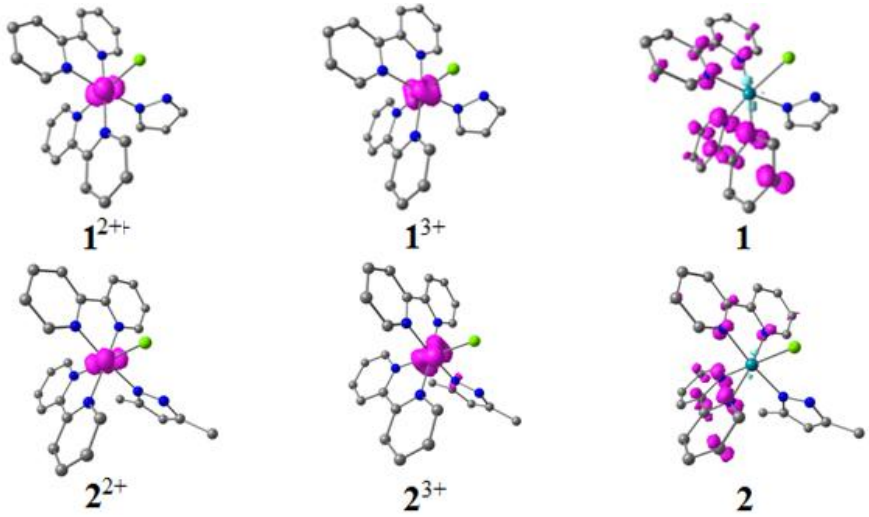

Fig. S2 DFT calculated Mulliken spin density plots for paramagnetic forms of $\mathbf{1}^n$ and $\mathbf{2}^n$.

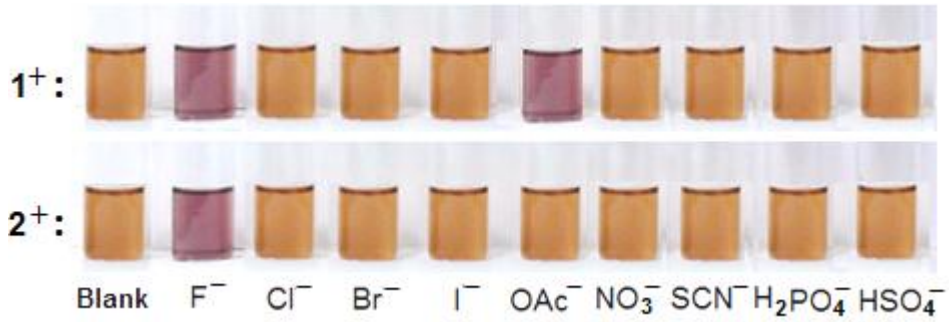

Fig. S3 The visual change in colour of **1**$^+$ and **2**$^+$ ($5x10^{-5}$ mol dm^{-3}) in CH_3CN on addition of eight equivalents of the TBA salt of anions.

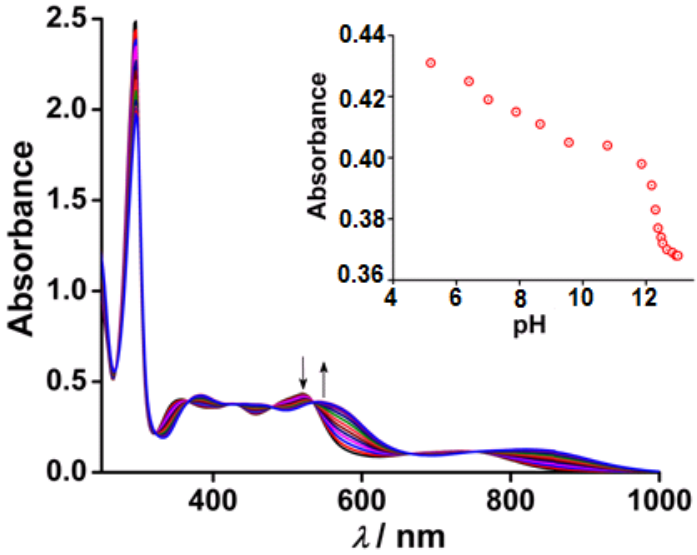

Fig. S4 Electronic spectra of **1**$^{+}$ as a function of pH in 1:1 CH_3CN-H_2O. Inset shows the change in absorbance at 520 nm with the pH.

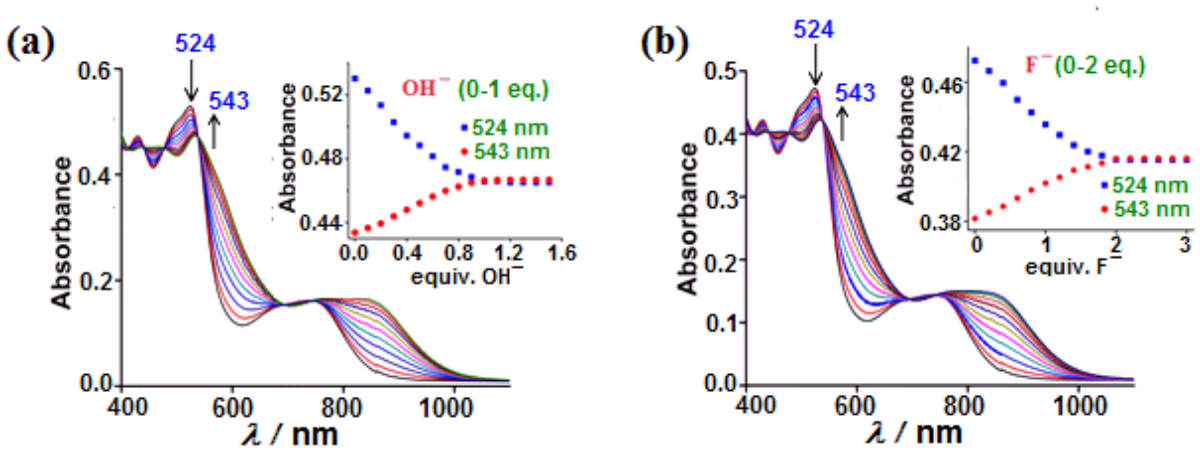

Fig. S5 UV-vis spectral changes of $\mathbf{2}^+$ ($5x10^{-5}$ mol dm^{-3}) in CH_3CN on gradual additions of (a) OH^- and (b) F^-. The insets show the changes in absorbance at 524 nm and 543 nm for OH^- and F^- as a function of the equivalents of respective anions.

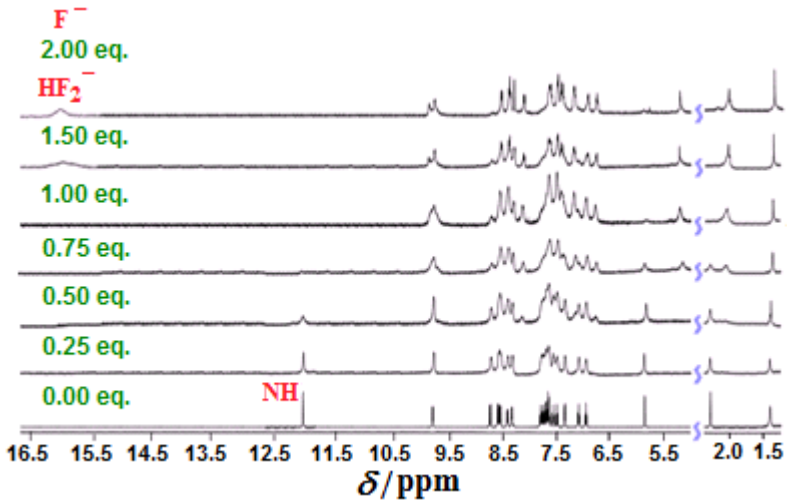

Fig. S6 ^{1}H-NMR titration of **2**$^{+}$ in $(CD_3)_2SO$ in presence of TBA salt of F^{-} ion (0-2 equivalents).

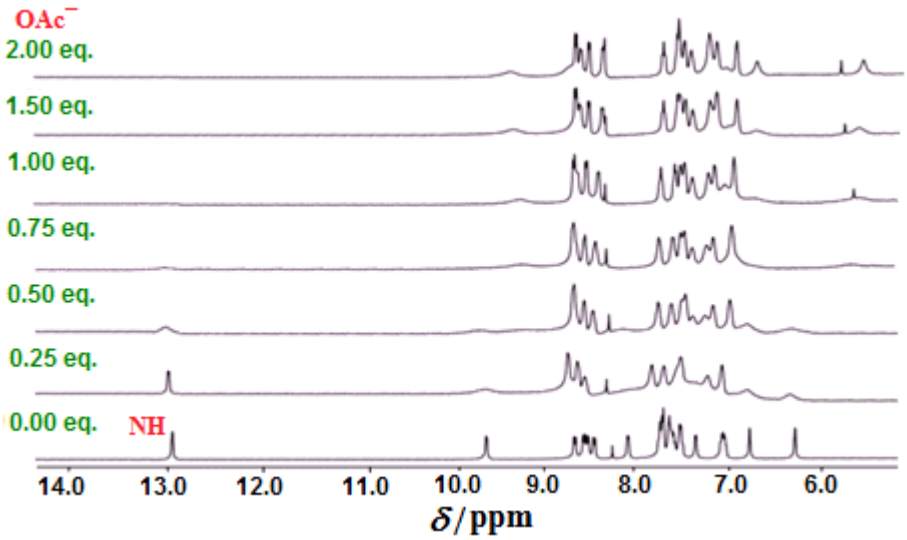

Fig. S7 ^{1}H-NMR titration of **1**$^{+}$ in $(CD_3)_2SO$ in presence of TBA salt of OAc^{-} ion (0-2 equivalents).

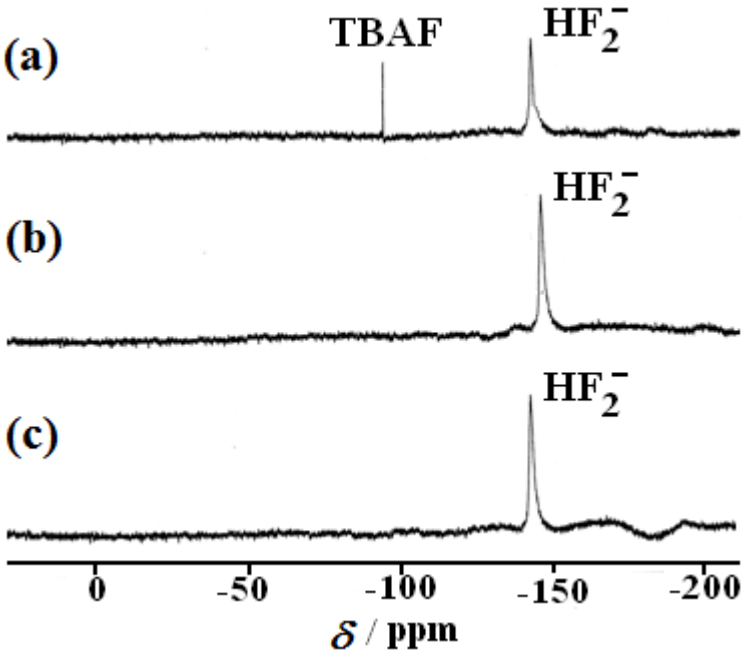

Fig. S8 ^{19}F-NMR spectra in $(CD_3)_2SO$ of (a) TBAF (b) TBAF in presence of one equivalent of **1**$^+$ and (c) TBAF in presence of one equivalent of **2**$^+$. Trifluoro-toluene is used as an internal standard ($\delta = -62.23$) at 298 K.

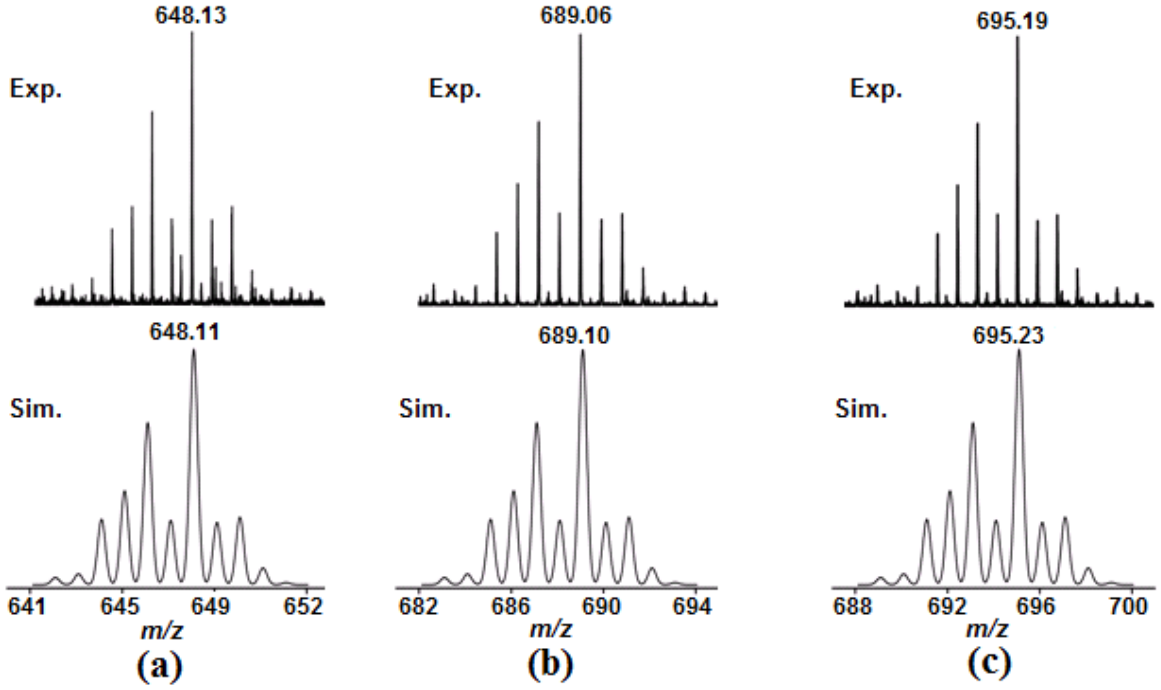

Fig. S9 ESI-MS in CH_3CN of *in situ* generated (a) [$\mathbf{1}^+$.F^-+Na^+], (b) [$\mathbf{1}^+$.OAc^-+Na^+] and (c) [$\mathbf{2}^+$.F^-+CH_3CN+H^+] by the addition of F^- and OAc^-, respectively, in the solution of $\mathbf{1}^+$ and $\mathbf{2}^+$.

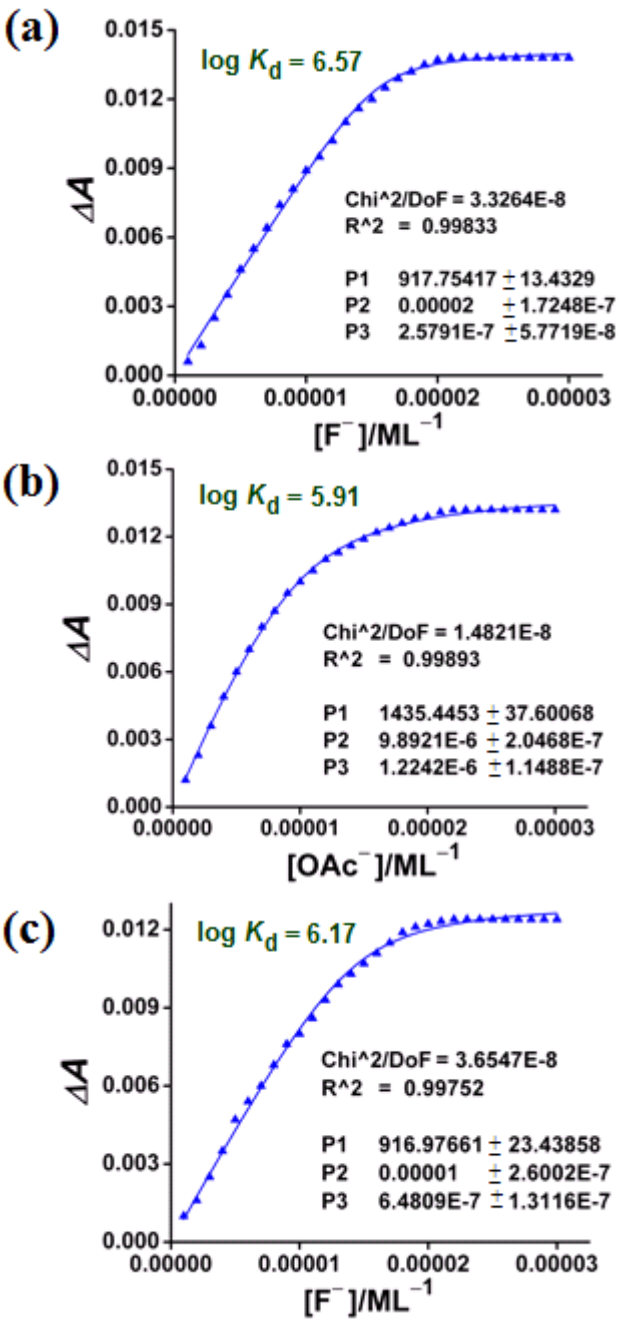

Fig. S10 Plots of the changes in absorbance (ΔA) in CH_3CN with respect to the initial absorbance of $\mathbf{1}^+$ (10^{-5} mol dm^{-3}) at 520 nm and $\mathbf{2}^+$ (10^{-5} mol dm^{-3}) at 524 nm on each addition of (a) F^-, (b) OAc^- and (c) F^- *versus* the concentration of the respective anions.

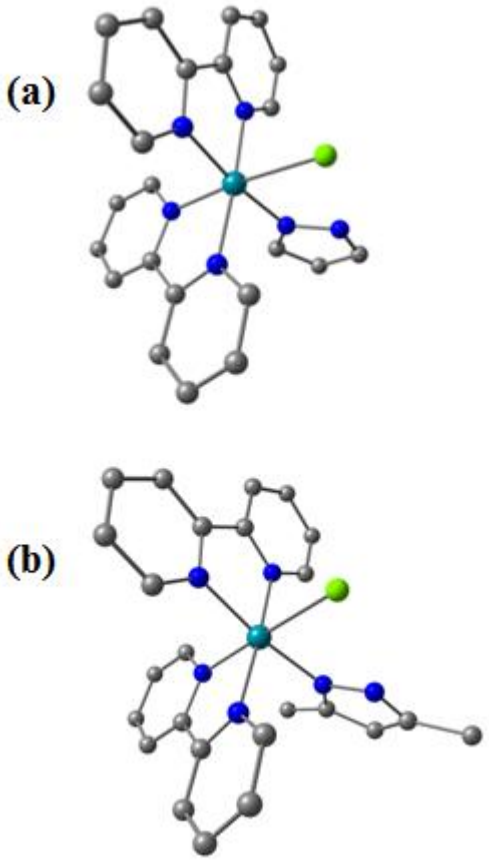

Fig. S11 DFT optimised structures of **1**$^{+}$ and **2**$^{+}$.

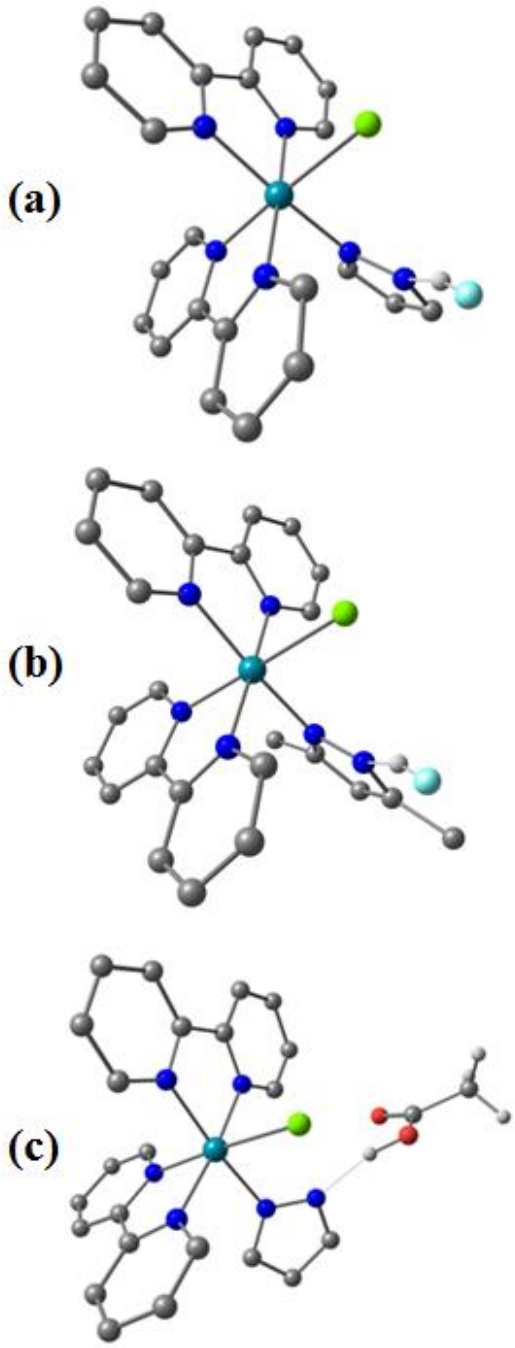

Fig. S12 DFT optimised structures of (a) [**1**$^{+}$···F^{-}] (**A)**, (b) [**2**$^{+}$ ···F^{-}] (**A**$^{/}$) and (c) [**1**$^{+}$···OAc^{-}] (**B**).